A new durable pigment with hydrophobic surface based on natural nanotubes and indigo: Interactions and stability

Guanzheng Zhuang, Maguy Jaber, Francisco Rodrigues, Baptiste Rigaud, Philippe Walter, Zepeng Zhang

A new durable pigment with hydrophobic surface based on natural nanotubes and indigo: interactions and stability

Guanzheng Zhuang [a,b], Maguy Jaber [a,*] Francisco Rodrigues [a,c], Baptiste Rigaud [d], Philippe Walter [a] and Zepeng Zhang [b]

[a] Sorbonne Université, Laboratoire d'Archéologie Moléculaire et Structurale (LAMS), CNRS UMR 8220, case courrier 225, UPMC 4 Pl. Jussieu, 75005 PARIS CEDEX 05, France.

[b] Beijing Key Laboratory of Materials Utilization of Nonmetallic Minerals and Solid Wastes, National Laboratory of Mineral Materials, School of Materials Science and Technology, China University of Geosciences, Xueyuan Road, Haidian District, Beijing 100083, PR China.

[c] Chemistry Department of State University of Paraiba (UEPB), Center of Science and Technology (CCT), Av. Juvêncio Arruda, s/n - Universitário, Campina Grande 58109-790, Paraiba, Brazil.

[d] Sorbonne Uniersité, CNRS Institut des Matériaux de Paris Centre (FR2482), 4 place jussieu, 75005 Paris, France.

Corresponding Author:

Maguy Jaber

Email: maguy.jaber@upmc.fr

Abstract

Covering with polyorganosilane (POS) was proved as an effective way to enhance the chemical and thermal stability of clay/dye hybrid pigments. But the photostability and interactions with clay minerals, dyes and POS layer has never been reported. In order to investigate above issues, new organic-inorganic hybrid pigments based on halloysite (Hal) and indigo (In) were prepared by grinding method. X-ray diffraction, transmission electron microscopy, thermogravimetry, Fourier transform infrared spectroscopy were applied to characterize the structure of In-Hal (without POS layer) and In-Hal-POS (with POS layer) pigments. Solid state nuclear magnetic resonance (NMR) was employed to reveal the interactions between Hal, In and POS. Reflection spectra and CIE 1976 color space system were used to evaluate the color parameters and color changes of pigments. Thermal stability, chemical resistance to ethanol, 1 mol·L^{-1} HCl and 1 mol•L^{-1} NaOH, and light fastness to visible light were tested. Indigo molecules dispersed on the surface of Hal nanotubes. POS layer homogeneously covered on the surface of hybrid pigments, without changing the crystal structure and morphology of Hal. Covering with POS layer seldomly affect the color of hybrid pigments. However, In-Hal-POS exhibited better stability than In-Hal, due to hydrophobic surface which can prevent indigo molecules from chemical reactions and degradation. A new route was proposed to prepare organic-inorganic hybrid pigments, ignoring the interaction between dye molecules and substrates.

Keywords: hybrid pigments, clay minerals, organic dyes, chemical stability, photostability.

1. Introduction

Maya blue (MB) is a fantastic pigment which was extensively used in ancient times in Mesoamerica. The MB was nearly extended to all Mesoamerican cultures. Many Maya cultures were kept by MB in the forms of murals, figurines and decoration of buildings. MB keeps its color well after centuries of vicissitudes. The remarkable resistance to weather, light, acids, bases, heat, as well as biodegradation had attracted much attention from scientists and archeologists. MB was confirmed as a hybrid pigments of palygorskite and natural indigo dye [1-3]. In the past decades, many efforts were taken to reveal the structure and stabilization mechanism of MB [4-10]. The interaction between palygorskite and indigo is believed to result in the amazing stability of MB, but the real nature of the interaction is still controversial. The most acknowledged interactions encompass hydrogen bonding, van der Waals forces, steric shielding and interaction between indigo and octahedral cations of palygorskite [3].

Despite the controversial mechanism, MB pigments provides a strategy of inorganic-organic hybrids to enhance the stability of organic dyes in applications. Many scientists tried to re-create the MB and MB-like pigments by using clay minerals and dyes. Adsorption in solvents and grinding in solid state were taken. A serious MB-like pigments with different colors were prepared using natural or synthetic dyes (such as methyl red, alizarin, murexide, Sudan red, cationic red X-GRL, methylene blue, and methyl violet etc.) [11-15]. Palygorskite [13, 14, 16], sepiolite

[17-20] and zeolite [21] were used as the matrix of hybrid pigments because of the nanosized porous structure which may accept more dye molecules and interact with each other. Besides, montmorillonite was reported as the matrix to prepare hybrid pigment by intercalating the dyes into the interlayer space [22-24]. These hybrid pigments, however, exhibited inferior stability to the ancient MB. In addition, the previous literature mostly concerned about the chemical stability of the hybrid pigments, but ignored the photostability, which is very important for the conservation of colorful products, especially for arts and constructions.

Herein, new substrates for hybrid pigments are considered. Halloysite (Hal) ($Al_2(OH)_4Si_2O_5 \cdot 2H_2O$) [25], a natural nanotubular clay mineral (see Fig. 1), is a promising host for organic-inorganic hybrid pigments. Generally, the length of halloysite nanotubes varies from ca. 0.02 to 30 μm and the external diameter from ca. 30 to 190 nm, with an internal diameter range of ca. 10-100 nm [26, 27]. The very large diameter of the halloysite lumen makes it potentially suitable for the accommodation of a range of guests. As a naturally occurring hydrated polymorph of kaolinite, it has a similar structure and composition, but the unit layers are separated by a monolayer of water molecules. Hydrated halloysite has a basal spacing (d_{001}) of 10 Å, which is ~3 Å larger than that of kaolinite. The interlayer water is weakly held, so that halloysite-(10 Å) can readily transform to halloysite-(7 Å) by dehydration. Tubular structure of halloysite results from the wrapping of the clay layers around onto themselves to form hollow cylinders under favorable geological conditions. This wrapping process is driven by a mismatch in the periodicity between the oxygen

sharing tetrahedral SiO_4 sheets and adjacent octahedral [$A1O_6$] sheets in the 1:1 layer.

The previous work about MB and MB-like pigments always concern about the interaction between dye molecules and clay substrates. However, the secret of MB has never been revealed by convincing evidences. Furthermore, hybrid pigments with the same stability to MB has not been re-produced by modern people. Another strategy to improve the stability of hybrid pigments, i.e., covering the hybrid pigment surface with a protective layer, should be considered. In this way, the interaction between dye molecules and substrates is insignificant. A substrate supports the dye molecules, which gives the color, and a protective layer packs the hybrid of substrates and dyes. Some attempts about a layer of silica [11, 28, 29] or polyorganosilane (POS) [30-33] covering the hybrid pigments surface were carried out. The authors confirmed that surface modification is an effective method to improve the stability of pigment. Particularly, hybrid pigments with a POS layer showed excellent chemical and thermal stability. The colorimetric properties, chemical and heat resistance are very significant for arts, architectures, industrial and daily products. In the literature, the chemical and thermal stability of hybrid pigments were discussed, however their photostability and the interactions between clay minerals, dyes and POS layer have never been revealed.

In this work, Hal was employed as a new substrate due to its nanotubular structure and large specific surface area. Indigo was chosen as the color giving agent. Polycondensation between two different organosiloxanes occurred on the surface of the hybrid of Indigo/Hal, and finally resulted in a protective layer. In comparison, the

hybrid pigment without covering with POS was also prepared. The structure, thermal stability, chemical resistance and photostability of these pigments were characterized to verify this new strategy for preparing durable hybrid pigments. What is more important, the interaction among Hal, indigo and POS was investigated.

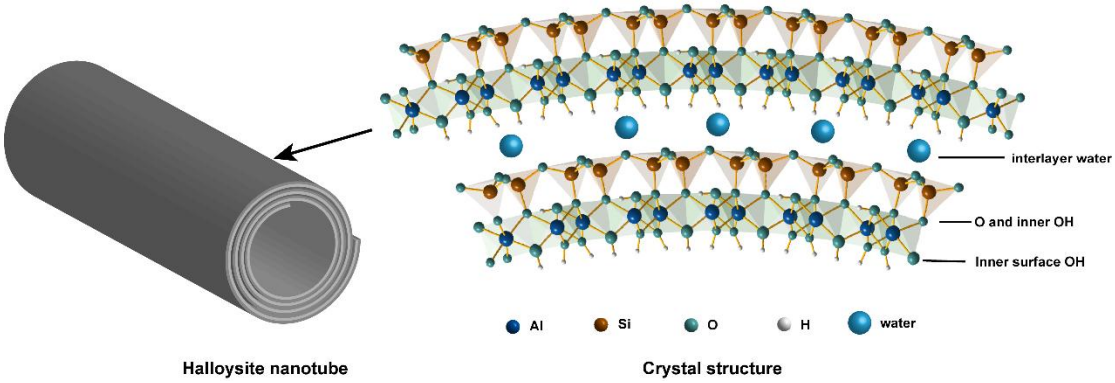

Fig. 1 The structure of halloysite.

2. Materials and methods

2.1 Materials

Hal, indigo (abbreviated as 'In' in the names of pigments), n-hexadecyltrimethoxysilane (HDTMS, purity of 85%) tetraethoxysilane (TEOS, purity of 99%) were purchased from Sigma-Aldrich, Inc, France. These materials were used without further purification. HCl (37%), NaOH (98.8%) and ethanol (95%) were purchased from VWR Co. Ltd. NaOH solution (1 mol·L^{-1}) was prepared by dissolving NaOH solids into water. HCl solution (1 mol·L^{-1}) was prepared by diluting concentrated HCl.

2.2 Preparation of hybrid pigments

In-Hal pigment was obtained by grinding halloysite and indigo (2% of the mass of halloysite) together in an agate mortar by hand for 20 min (Fig. 2 (A)). Then, In-Hal-POS pigment were prepared by polycondensation of HDTMS and TEOS in the presence of In-Hal pigment (Fig. 2 (B)). 0.50 g of the In-Hal pigment was fully dispersed in 9 mL of ethanol and 1 mL of ammonia saturated ethanol, magnetically stirring for 3 min in a vial. Then, proper amounts of TEOS and HDTMS (concentration of 0.15 mol•L^{-1}) were charged into the mixture with stirring. The dispersion was ultrasonicated for 30 min at 50 °C, and then 1.44 mL of water was injected quickly into the dispersion under ultrasonication. The vial was sealed and ultrasonicated at 50 °C for 1 h. The products were centrifuged at 6000 rpm for 5 min to remove the supernatant followed by washing 3 times each with ethanol. Then, the hydrophobic In-Hal-POS pigment was obtained after drying at 50 °C for 24 h.

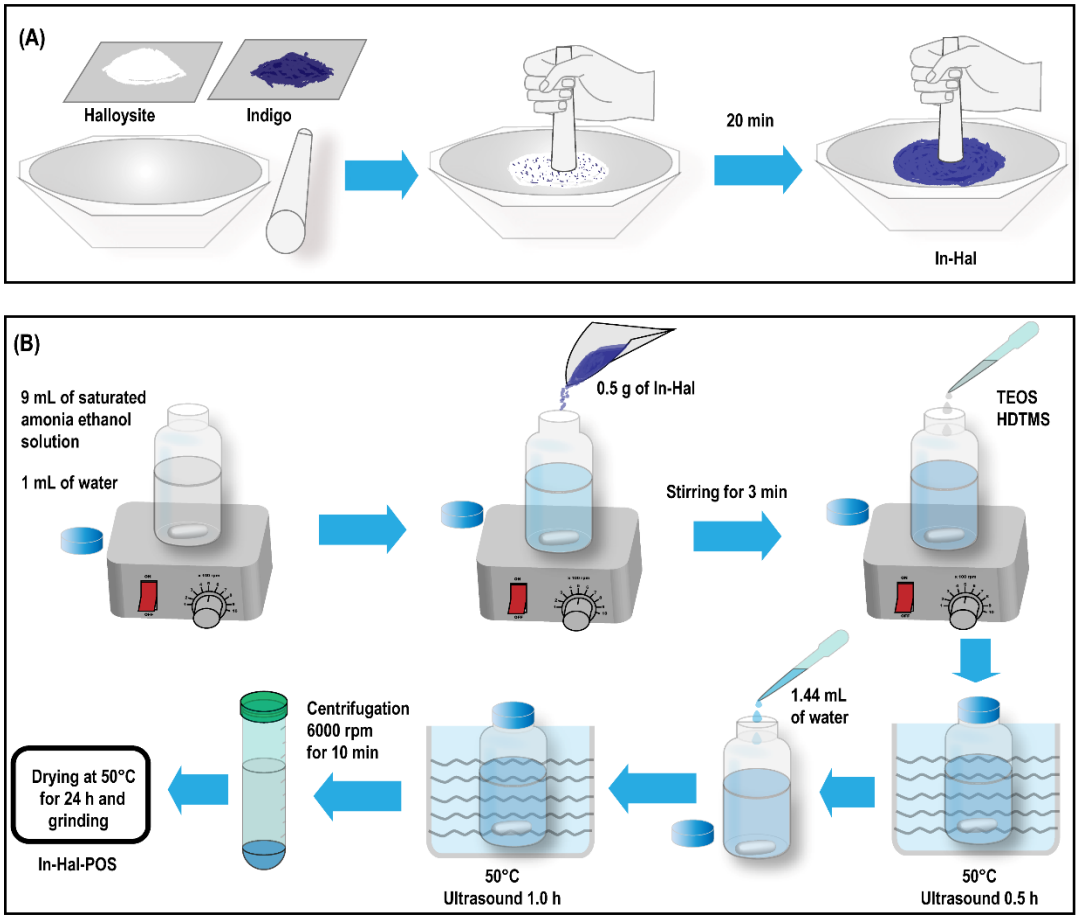

Fig. 2 Experimental procedure to prepare (A) In-Hal and (B) In-Hal-POS pigments.

2.4 Characterization

X-ray diffraction (XRD) test was conducted at a Bruker D8 diffractometer from 5° to 70° at a speed of 4 s per step (step size of 0.02°). Fourier transform infrared (FTIR) spectra were collected from a Cary 630 FTIR spectrometer in the range of 4000-650 cm^{-1}. Thermogravimetric (TG) analysis was carried out at a TA-SDTQ600 type analyzer from room temperature to 900 °C in the air atmosphere, with the heating rate of 10 °C/min. Transmission electron microscopy (TEM) was performed on a Tecnai Spirit G2 transmission electron microscope with the voltage of 120 kV. The samples were dispersed in ethanol with ultrasound for 30 min, then the dispersions were dropped on copper supports with carbon grid.

^{13}C, ^{1}H and ^{27}Al Magic angle spinning (MAS) nuclear magnetic resonance (NMR) spectra were obtained on a Bruker Advance III spectrometer equipped with a 2.5 mm and 4 mm H-X MAS probe, operating at frequency of 500.07 MHz (^{1}H), 125.76 MHz (^{13}C), 99.36 MHz (^{29}Si) and 130.30 MHZ (^{27}Al). Chemical shifts were calibrated using the carboxyl signal of adamantane (38.52 ppm) for ^{13}C and (1.85 ppm) for ^{1}H, TMS (0 ppm) for ^{29}Si and $Al(NO_3)_3$ (0 ppm) for ^{27}Al as external standard. The ^{1}H experiment using 90° pulse was recorded with a spinning rate of 14 kHz, with a number of scans of 128 and 1 s of recycle delay. The ^{13}C Cross-Polarization spectra were acquired with a MAS rate of 14 kHz, a ramp-CP contact time of 2 ms and a 2 s of recycle delay and with a ^{1}H decoupling spinal. Over an acquisition time of 40 ms, the number of scans to obtain the spectra depends on the S/N obtained for each sample. Spectra were processed with a zero-filling factor of 2 and with an exponential decay corresponding to a 10 Hz line broadening in the transformed spectra. Only spectra with the same line broadening are directly compared. The ^{27}Al experiment using 30° pulse was recorded in the same condition of spinning rate (14 kHz), with a number of scans of 2048, 263 kHz spectral width and with 500 ms of recycle delay. The ^{29}Si experiment using 90° pulse with a ^{1}H decoupling spinal was recorded in exactly the same condition of spinning rate. The number of scans was 8192 and the recycling time D1 was 10 s. The Spectra were processed with a zero-filling factor of 2 and without an exponential decay.

The absorbance, reflectance and CIE (Commission Internationale de L'Eclairage) parameters were obtained from an Ocean Optics spectrometer USB4000. The light

source of Ocean Optics DH-2000-BAL was used for absorbance, and HL2000 light source was employed for reflectance and CIE results. CIE 1976 color space system was applied to evaluate the color of the pigments. Lightness (L*) represents the brightness (+) or darkness (-) of the color, i.e., more positive L* values refer to whiter while more negative L* values represent darker. The values of a* and b* indicate the color details: +a* is the red direction, -a* the green direction, +b* the yellow direction, and -b* the blue direction. Before the reflectance and CIE test, the samples were pressed into tablets with the pressure about 30 MPa. The total change in color was calculated as $\Delta E^* = \sqrt{(L_1^* - L_0^*)^2 + (a_1^* - a_0^*)^2 + (b_1^* - b_0^*)^2}$, where L_1* refers to the L* value of a sample, L_0* refers to the L* value of the reference, and similar to the other two parameters. Thermal stability of hybrid pigments was tested by calculating the total color change between raw pigment and that heated at high temperatures for 4 h. Photostability was evaluated under visible lights for 360 h using an Advanced Illumination SL164 type LED light. The working distance between the light and the samples is 10 cm, corresponding to a diameter of 3.6 cm of working area, with the illuminance of 50 kLux. Hence, the fading test applied for the prepared hybrid pigments gave a total light dose of 18000 kLux·h (50 kLux × 360 h). This light dose equals to about 30 years in a common museum gallery illuminated at 200 Lux (10 h of light exposure per day, 6 days per week, and 50 weeks per year). Similar calculation can be found in the literature [34, 35]. To avoid the influence of humidity and temperature, the tableted pigments were placed in a special apparatus (see Fig. 3) with desiccants at 20 °C.

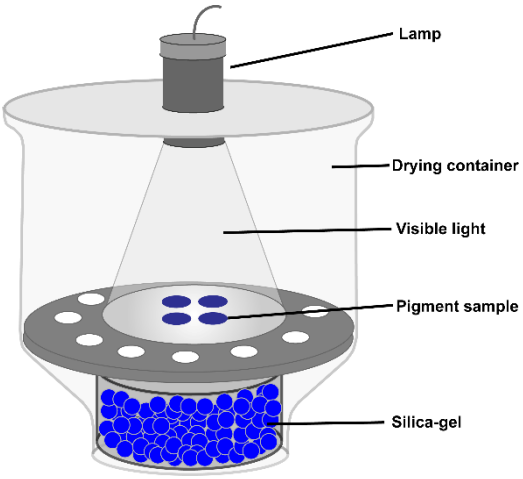

Fig. 3 The apparatus for photostability test.

3. Results and discussion

3.1 Structure and morphology

The XRD pattern of Hal (Fig. 4) exhibits the typical reflections of halloysite, with a little amount of quartz and albite. Hal shows a basal spacing of 0.75 nm, demonstrating a dehydrated halloysite. In-Hal and In-Hal-POS pigments present the similar XRD patterns with the raw Hal, without any change of the basal spacing. This phenomenon indicates that indigo molecules did not intercalate into the interlayer space of halloysite. XRD pattern of indigo proves a crystalline structure of indigo solid. But no reflection belonging to indigo crystals was observed in the XRD patterns of hybrid pigments. This fact demonstrates that indigo molecules re-organized on the surface (including external and inner surface) of hybrid pigments. As Fig. 5 shows, halloysite exhibits the tubular morphology. The length of Hal nanotubes ranges from dozens to hundreds of nanometers. Hal shows an inner diameter of more than 10 nm.

Although the indigo molecules cannot insert into the interlayer space, they can stay on both the external and inner surface. In-Hal hybrid pigment shows the similar morphology with Hal. Covered with POS, In-Hal-POS pigment still exhibits the tubular morphology and similar surface. This fact indicates that polycondensation between TEOS and HDTMS happened homogeneously on Hal surface, uniformly embedding indigo molecules and Hal.

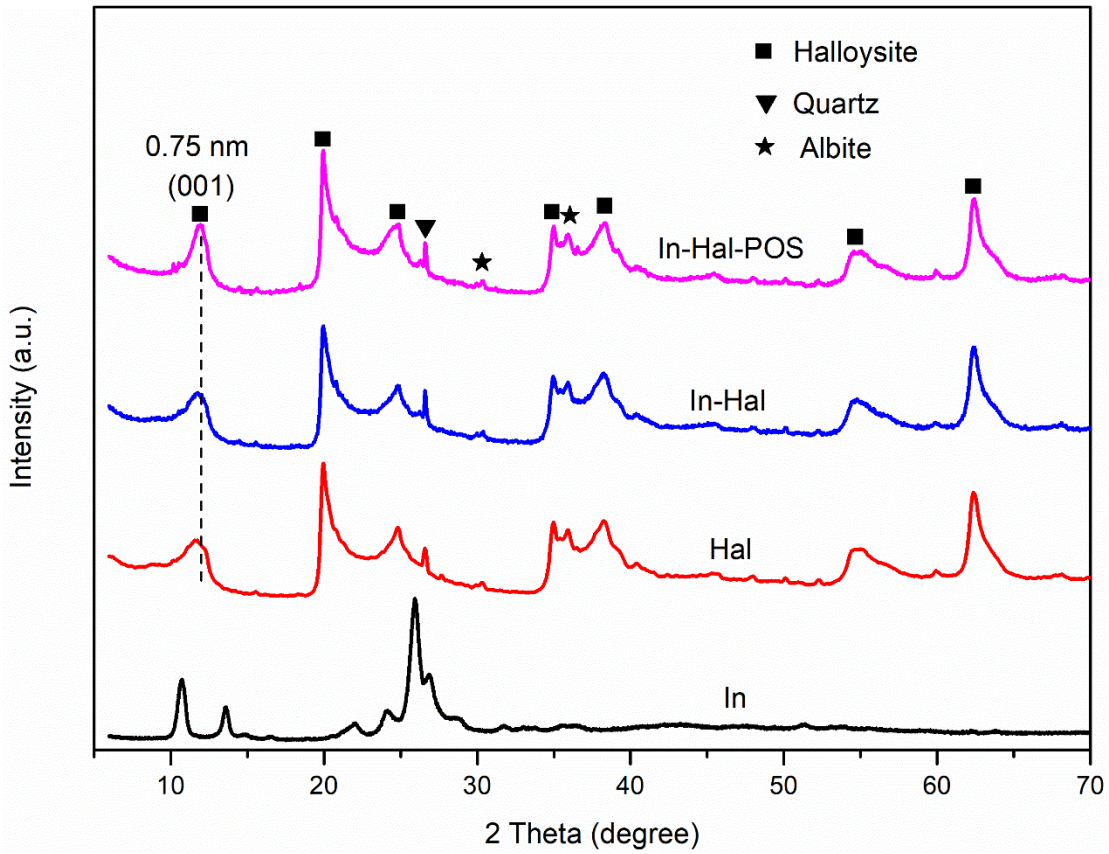

Fig. 4 XRD patterns of (A) Hal and hybrid pigments and (B) indigo.

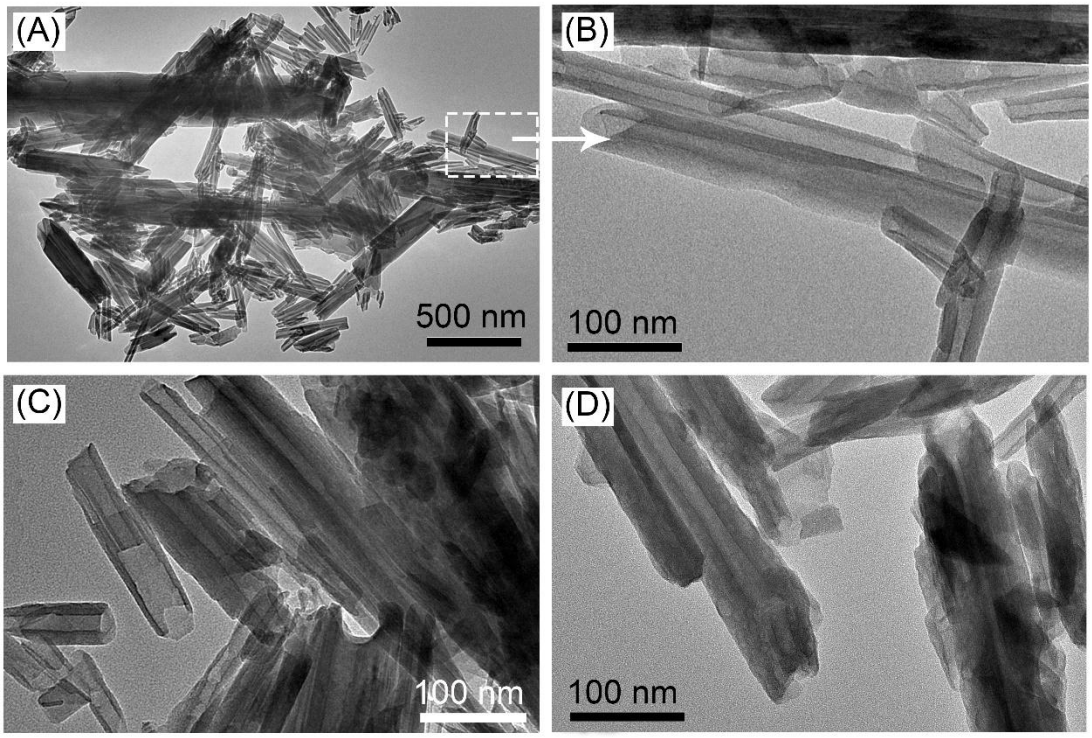

Fig. 5 TEM images of (A) and (B) Hal, (C) In-Hal and (D) In-Hal-POS.

The TG and corresponding derivative TG (DTG) curves of Hal, Indigo and hybrid pigments are displayed in Fig. 6. Hal presents three steps of mass loss. The mass loss before 120 °C, corresponding to the DTG peak at 56 °C, is attributed to the loss of adsorbed water on the Hal surface [36, 37]. The small mass loss at the 152 °C (DTG peak) is due to the mass loss of the small amount of interlayer water [38]. Although XRD pattern demonstrates a dehydrated Hal, the wide (001) reflection proves a little interlayer water remains. The adsorbed and interlayer water amount is about 3.5%. The third step at the range of 350-600 °C, corresponding to the DTG peak at 485 °C, is assigned to the dehydroxylation of Al—OH and Si—OH groups [37-40]. The oxidation of indigo starts at about 350 °C. Continuous oxidation goes until 580 °C. In-Hal exhibits the similar TG and DTG curves with raw Hal. It is difficult to

distinguish the oxidation process of indigo dyes in In-Hal sample, due to the overlap of dehydroxylation process. But 2% more mass loss above 300 °C of In-Hal than Hal indicates the including of indigo in the hybrid pigment. In the TG and DTG curves of In-Hal-POS, a new mass loss step at the range of 300 to 400 °C emerged, with the mass loss of 9.9%. This is assigned to the thermal decomposition of POS which covers the surface of hybrid pigment. Continuous oxidation of POS at higher temperatures mixes with the dehydroxylation of Hal and oxidation of indigo, resulting in the mass loss of 15.2%.

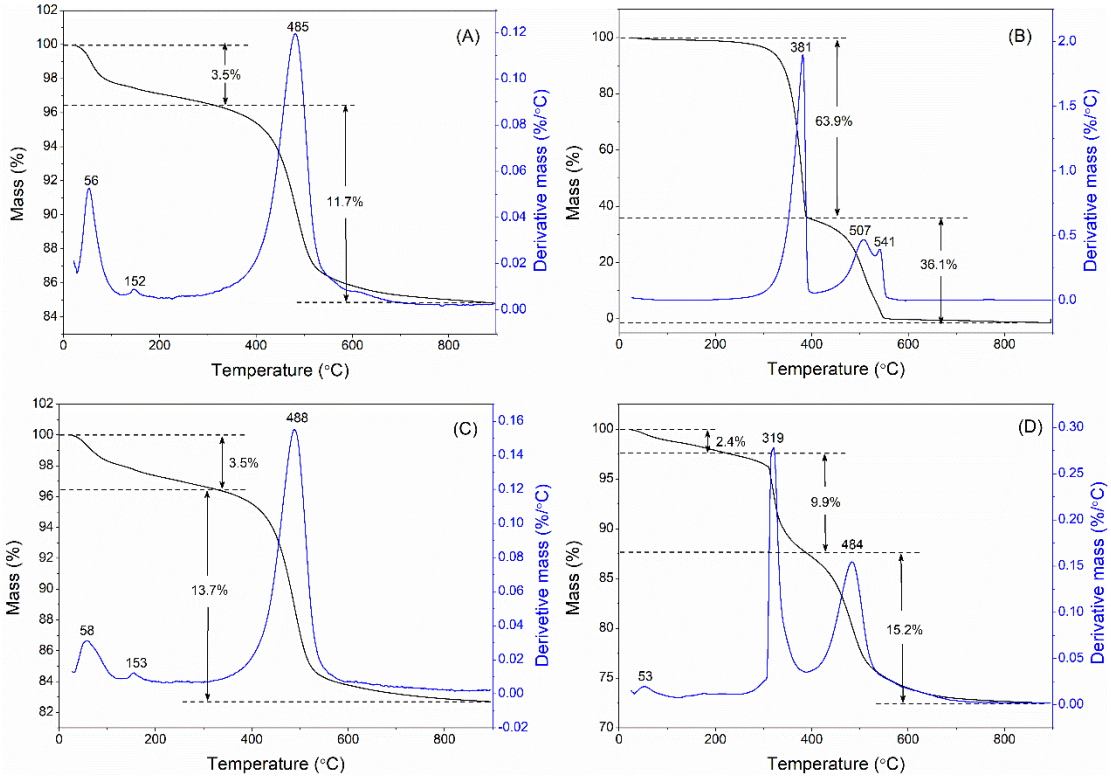

Fig. 6 TG and DTG curves of (A) Hal, (B) indigo, (C) In-Hal and (D) In-Hal-POS.

3.2 Solid state NMR

^{13}C MAS NMR spectra of indigo and hybrid pigments are presented in Fig. 7. The

signals of indigo occur in the chemical shift range of 100-200 ppm. Indigo, In-Hal and In-Hal-POS exhibit the similar signals in this range. The only difference is the lower intensity of In-Hal and In-Hal-POS than the bulk indigo, because of the less content of indigo in the hybrid pigments. Compared with the spectra of indigo and In-Hal in the range of 10-60 ppm, some newly emerged signals are observed. These signals are from the POS and the assignments are marked. The ^{13}C chemical shifts of TEOS appear at 18.4 and 58.9 ppm, and correspond to $–CH_2CH_3$ group. Although these two signals are absent in the ^{13}C spectra of In-Hal-POS, indicating that TEOS was completely hydrolyzed and/or condensed. The signals from HTDMS alkyl chain are observed (10-40 ppm), demonstrating the successful immobilization of POS. A weak signal at 50.6 ppm, is assigned to methyl groups connected with O—Si groups in HTDMS, indicating that a few HTDMS molecules were not hydrolyzed completely. Hence, most $Si—OCH_3$ groups in HTDMS were hydrolyzed and finally condensed into POS.

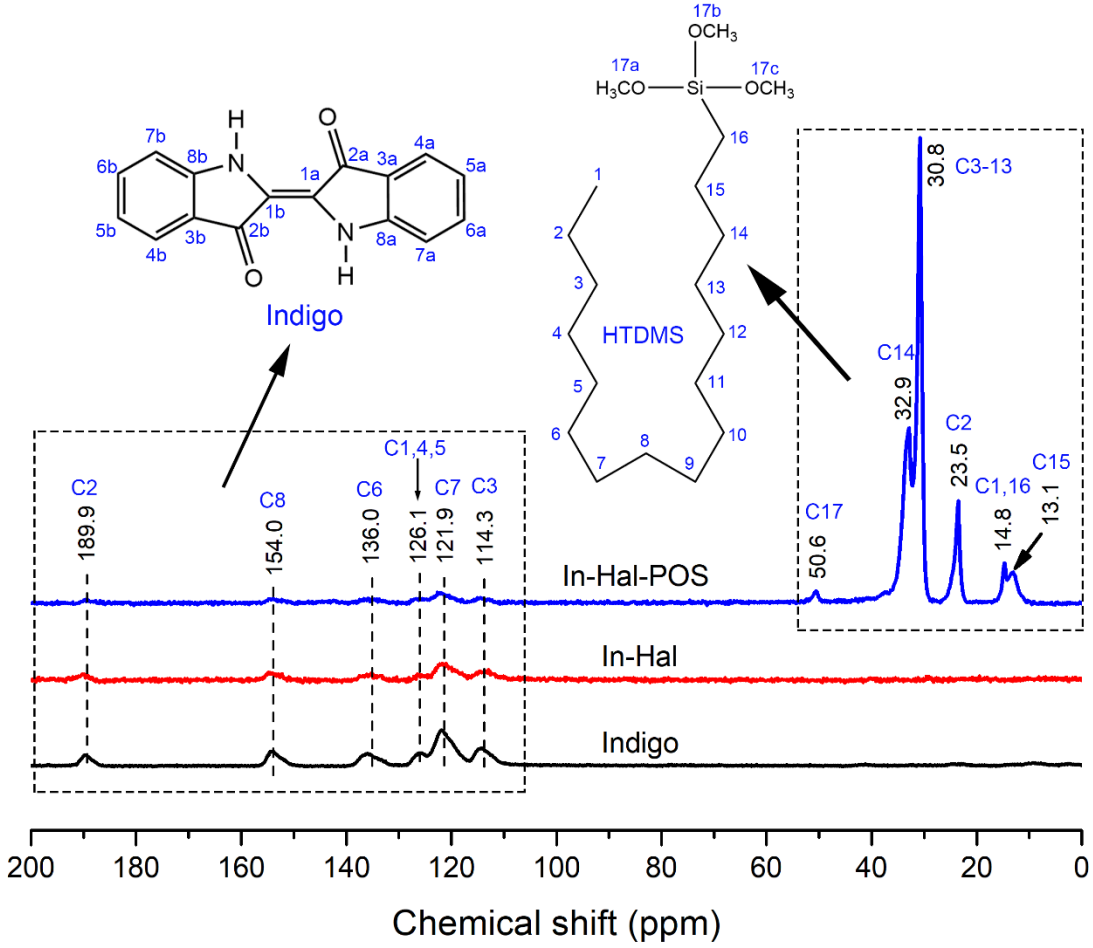

Fig. 7 ^{13}C MAS NMR spectra of indigo, In-Hal and In-Hal-POS.

^{1}H MAS NMR spectra of the materials and hybrid pigments (Fig. 8) reveal the chemical interaction changes. The signal of indigo is composed of four signals, i.e., signal at 1.4 ppm corresponding to C—H of methyl group (indicating some impurities), 4.6 ppm indicating some adsorbed water, 7.2 ppm representing the C—H groups and 10.6 ppm tracing the N—H groups of indigo [41]. The signal of Hal can be also decomposed into two signals at 4.6 ppm (water) and 2.3 ppm (—OH groups). In-Hal shows the similar spectrum with Hal, except for a more intense and sharper signal at around 2.3 ppm. The ^{1}H MAS NMR spectra of In-Hal can be decomposed

into four individual signals, i.e., 7.3 ppm, 4.6 ppm, 2.3 ppm and 2.2 ppm. The signal at 7.3 ppm corresponds to the C—H groups from indigo. The signals at 4.6 ppm and 2.3 ppm are assigned to water and –OH groups in Hal, respectively. The N—H signal disappeared while a new signal emerged at 2.2 ppm, very close to the signal of –OH. This phenomenon demonstrating the interaction happened between N—H groups and Hal. Indeed, it is possible that hydrogen bonds can be formed between the N—H groups and Si—O or Al—O groups. Consequently, the chemical shift decreased to 2.2 ppm. The ^{1}H MAS NMR spectrum of In-Hal-POS can be decomposed into 6 signals. Signals at 1.0 ppm, 1.5 ppm and 3.6 ppm are attributed to C—H groups of organosilanes. Signal at 2.1 ppm is assigned to the –OH groups of Hal and hydrogen bonged N—H groups. The signal at 4.6 ppm is attributed to water. Weak signal of C—H groups from indigo at 7.2 ppm is also noticed.

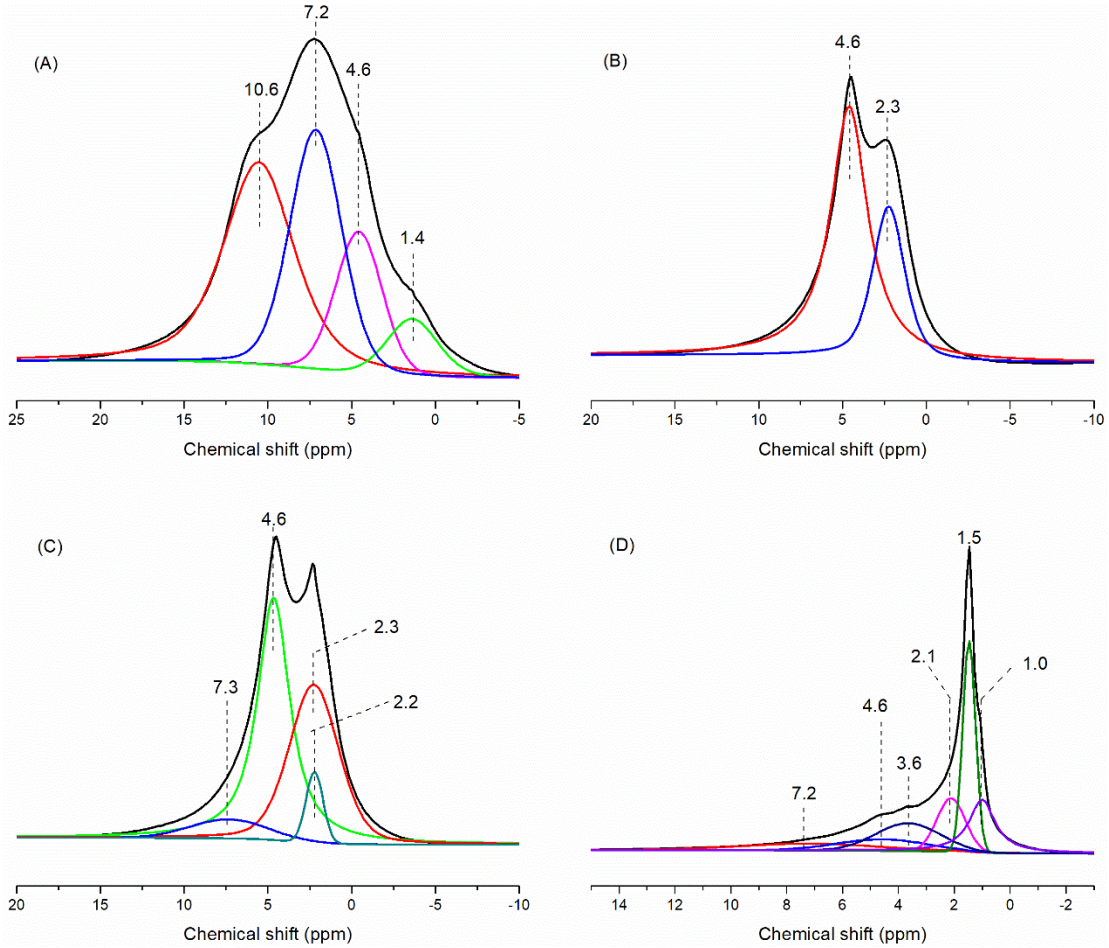

Fig. 8 ^{1}H MAS NMR spectra of (A) indigo, (B) Hal, (C) In-Hal and (D) In-Hal-POS.

^{27}Al MAS NMR spectra (Fig. 9 (A)) show two signals representing sixfold coordinated Al (δ = 4.8 ppm, marked as Al(VI)) and fourfold coordinated Al (δ = 50-80 ppm, marked as Al(IV)), very close to the previous literature [42, 43]. Usually, Al locates in the center of [AlO_6] octahedra. Al(IV) occurs due to the substitution of Si^{4+} in [SiO_4] by Al^{3+}, and finally form some [AlO_4] tetrahedra defects. About 5% of Al(IV) and 95% of Al(VI) are evaluated by integration. The hybrid pigments show similar Al(VI) signals to raw Hal, i.e., 4.8 ppm, demonstrating that indigo did not affect the Al coordination in the Hal. The Al(IV) signal of Hal occurs at 69.3 ppm. But

the Al(IV) chemical shift of In-Hal hybrid pigment decreases to 68.0 ppm. This change may be caused by the hydrogen bonds between Al—OH (Hal) and C=O (indigo) groups or between Al—O (Hal) and N—H (indigo) or even Van der Walls force (see Fig. 9 (C)). The reaction between Hal and indigo reduce the electron density of Al, resulting in the shift of chemical shift to high fields. The Al(IV) spectrum of In-Hal-POS can be decomposed into two signals, i.e., 68.0 ppm and 55.6 ppm. Signal at 68.0 ppm is very close to the signal of that of In-Hal. Hence, the chemical shift of 68.0 represents the Al atoms connected with indigo via hydrogen bonds. The shift to higher field at 55.6 ppm indicates the increase of electron density of some Al atoms. Compared with the raw Hal, the large shift ($\Delta\delta$ = 13.7 ppm) suggest strong chemical reaction. The most possibility is the polycondensation between the Al-OH and Si-OH (derived from the hydrolysis of organosilane), resulting in Al-O-Si groups. Previous work [40, 44-47] also reported the surface modification of Hal by grafting with organosilane. Condensation between Si—OH (from organosilane) and Si—OH or Al—OH groups resulted in chemical connection between organic modifiers and Hal surface.

The Al(IV) NMR signals demonstrate the hydrogen bond between Hal external surface and indigo, and condensation reaction between Hal external surface and organosilanes. The ^{29}Si MAS NMR spectra (Fig. 9 (B)) of Hal, In-Hal and In-Hal-POS also testified the condensation between organosilanes and Hal external surface. The chemical shift at -91.2 ppm is assigned to the Q^3 silicon, $Si(OSi)_3(OH)$, of Hal [40, 48]. Five signals at -110.8, -78.2, -64.8, -55.8 and -48.7 ppm are

distinguished by Gauss deconvolution. According to the previous reports [40, 48, 49], they are attributed to Q^4, Q^2, T^3, T^2 and T^1 silicon, respectively (see Fig. 9 (D)). The integral areas of these three signals follow as $Q^4 > T^3 > T^2 > T^1 > Q^2$, demonstrating multiple branches of POS. Accordingly, Q^3 silicon should be also generated, but the signal is overlapped by the Q^3 silicon signal of halloysite. This evidence proves the hyperbranched structure of POS. Organosilanes also bonded to the surface of Hal because of the Si—OH and Al—OH groups, as the ^{27}Al MAS NMR results proved. The connection between organosilanes and Si—OH groups also contributes to the Q^4 signal.

In summary, indigo molecules interact with the Hal external surface via hydrogen bonds between N—H groups and Si(Al)—O. But the Van der Waals force between the other groups and Hal should not be neglected. POS works as a dense protective layer by forming hyperbranched structure. POS can not only simply cover on the surface of hybrid pigments, but also bond to Hal surface by condensation reaction.

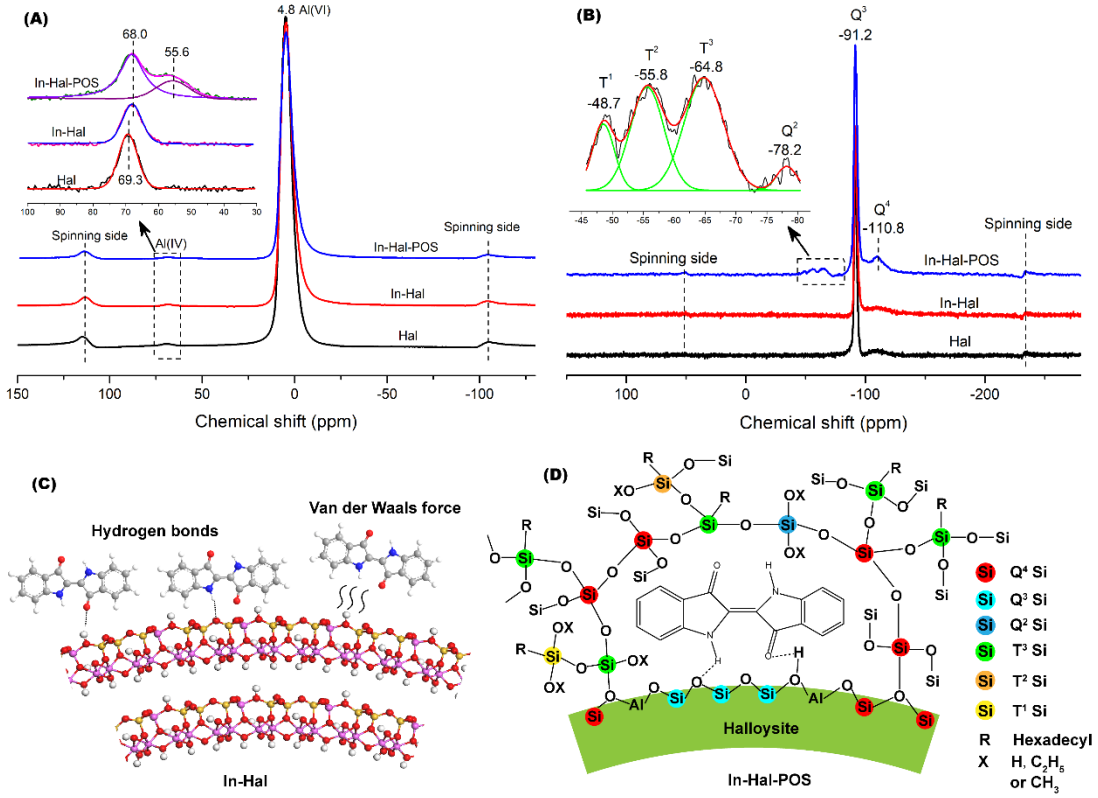

Fig. 9 (A) ^{27}Al and (B) ^{29}Si MAS NMR spectra of Hal and hybrid pigments; (C) schematically interpretive diagrams of interaction between indigo and Hal external surface; and (D) the structure of POS.

3.3 Color of hybrid pigments

Both In-Hal and In-Hal-POS pigments show the similar colors and reflection spectra (Fig. 10). The dominant reflections lie at 437 nm for In-Hal and 425 nm for In-Hal-POS, indicating the blue colors, in agreement with the digital pictures. The CIE parameters of In-Hal and In-Hal-POS are listed in Table 1. The low negative b* values and a* values which are close to zero indicate the blue colors. In addition, the similar L*, a* and b* values of In-Hal and In-Hal-POS also prove the similar chroma parameters of these two hybrid pigments. Hence the covering with POS layer did not

change the color of hybrid pigments a lot.

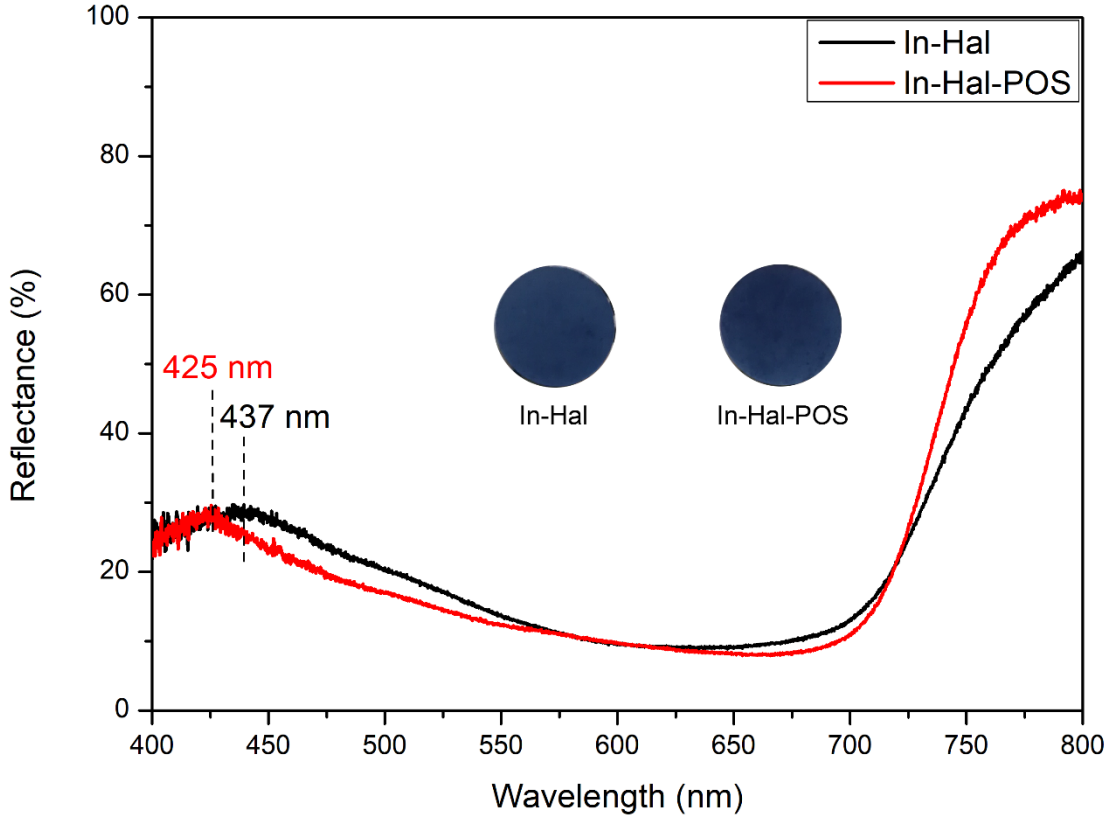

Fig. 10 Reflectance spectra of In-Hal and In-Hal-POS hybrid pigments, with the inserted digital pictures.

3.4 Thermal stability of the hybrid pigments

The CIE parameters of In-Hal and In-Hal-POS pigments heated at different temperatures are listed in Table 1. In-Hal pigment shows the L* value of 44.1, a* value of -1.1 and b* of -23.9, indicating the blue color. After heating to 190 °C, the brightness of pigments increased with the L* value of 54.2, demonstrating the shift to brighter. In addition, the larger negative a* and smaller negative b* values of In-Hal

heated at high temperature prove the color changes to greener and less blue. Heated at high temperatures, In-Hal-POS also shifts to brighter, greener and less blue, but the color differences are different. △E* values is an indicator of the color change of the pigments heated at different temperatures. In-Hal shows the △E* value of 3.0 at 150 °C, 8.9 at 170 °C and 17.1 at 190 °C, compared with the raw In-Hal pigment. Nevertheless, In-Hal-POS presents a better thermal stability with the △E* value of 3.7 at 150 °C, 5.8 at 170 °C and 11. 8 at 190 °C in comparison with the raw In-Hal-POS. The smaller△E* values of In-Hal-POS heated at high temperatures demonstrate the better thermal stability of hybrid pigments with the covering of POS layer.

Table 1 The chroma parameters of hybrid pigments and the corresponding heated pigments.

Sample	Heating temperature (°C)	L*	a*	b*	△E*
In-Hal	Without heating	44.1	-1.1	-23.9	0.0
In-Hal-150	150	46.1	-3.1	-24.9	3.0
In-Hal-170	170	50.6	-6.4	-21.0	8.9
In-Hal-190	190	54.2	-6.9	-11.4	17.1
In-Hal-POS	Without heating	42.1	1.4	-21.8	0.0
In-Hal-POS-150	150	44.8	-1.2	-21.4	3.7

In-Hal-POS-170	170	45.0	-3.0	-19.5	5.8
In-Hal-POS-190	190	47.3	-6.2	-14.4	11.8

The phenomenon of changing to greenish color was also found in MB pigment. Antonio et al. [50, 51] reported oxidation of indigo in MB pigment and found the presence of dehydroindigo (the oxidized form of indigo) contributed the greenish color of Maya blue. The FTIR spectra (Fig. 11) reveal the structural changes of the hybrid pigment. The FTIR spectrum of Hal demonstrates the presence of inner-surface ―OH (3693 cm^{-1}), inner ―OH (3622 cm^{-1}) and surface adsorbed water (3548 cm^{-1}) [52-54]. The bands at 1652 cm^{-1} and 1632 cm^{-1} correspond to the bending vibration H_2O and -OH groups, respectively. The band at 1118 cm^{-1} is attributed to the bending vibration of apical Si―O groups. The bending in-plane of Si ―O―Si groups results in the two absorptions at 1019 cm^{-1} and 1008 cm^{-1} [53]. The bands observed at 940 and 906 cm^{-1} are caused by the O―H deformation of inner-surface hydroxyl groups, and O―H deformation of inner hydroxyl groups, respectively [40]. Indigo exhibits complex absorption bands. According to the previous literature [55-57], the FTIR absorptions can be assigned. The band at 3262 cm^{-1} is assigned to stretching vibration of N―H groups. The bending vibration of N ―H groups occur at 1389 and 1123 cm^{-1}. The band at 3059 cm^{-1} represents C―H from benzene ring. The absorption of C=O groups occur at 1623 cm^{-1} for stretching vibration and 1063 cm^{-1} for rocking. A group of bands at 1608, 1584, 1481 and 1460 cm^{-1} belong to the stretching vibration of C―C in benzene rings. The stretching bands

of C—N groups happen at 1389 and 1170 cm^{-1}. The bending vibrations of C—H and C—C groups emerge in the range of 1350-1100 cm^{-1}.

Compared with the raw Hal, Hal heated at 190 °C (Hal-190) exhibits the similar FTIR spectrum to Hal, except for the absorption band of H_2O. The bands at 3548 and 1652 cm^{-1} corresponding to the adsorbed H_2O disappeared in the FTIR spectrum of Hal-190. This phenomenon indicates that heating until to 190 °C for 4 h can only remove the adsorbed water of Hal. The heated indigo (Indigo-190) shows the same FTIR spectrum to raw indigo, demonstrating the stable structure of indigo at 190 °C. This result is in agreement with the TG result, which proves that the thermal decomposition of indigo happens at more than 300 °C. In-Hal hybrid pigment presents the mixed FTIR spectra of indigo and Hal. Compared with the FTIR spectrum of In-Hal, the heated samples present some shifts. Firstly, the band of H_2O (3548 cm^{-1}) disappeared, demonstrating the dehydration of Hal. In addition, the absorptions involving the N—H, benzene ring, C—H, C—N and C—C groups dramatically decrease in FTIR spectra of the heated In-Hal pigments. This fact suggests the serious degradation of indigo molecules in In-Hal pigment when being heat from 150 °C to 190 °C. Hence, the tendency of changing to green at high temperature is due to the oxidation of indigo molecules in hybrid pigments. Considering the thermal behavior of indigo, indigo is stable below 300 °C, implying two possibilities: (i) individual indigo molecules (without crystalline structure) exhibit worse thermal stability; and (ii) some groups in Hal promote the thermal decomposition of indigo at 1ower temperatures. The appearance of —CH_3 (2923

cm^{-1}) and —CH_2 (2851 cm^{-1}) groups, and the increase of absorption of Si—O—Si in the spectrum of In-Hal-POS, imply the presence of POS. The FTIR spectra of heated In-Hal-POS hybrid pigments show all the presence of chemical groups of indigo. Compared with the absorption intensity of In-Hal-POS, heated In-Hal-POS pigments nearly keep the same intensity of absorptions of indigo. It means most indigo molecules are stable in the hybrid pigment of In-Hal-POS even after being heated until 190 °C.

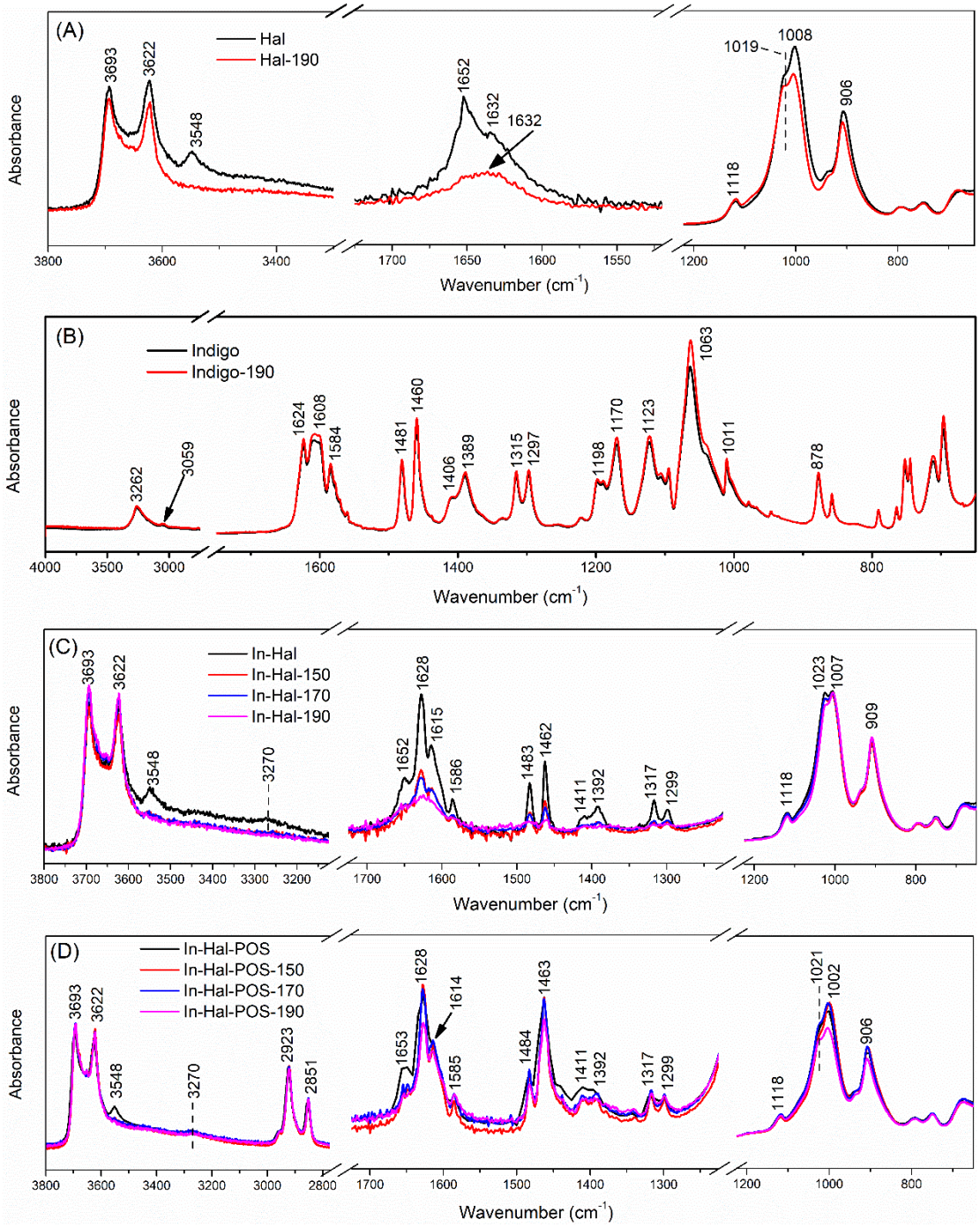

Fig. 11 FTIR spectra of (A) Hal and Hal-190, (B) indigo and indigo-190, (C) In-Hal hybrid pigments and (D) In-Hal-POS hybrid pigments.

3.5 Chemical stability

The hybrid pigments were treated by ethanol, HCl (1 mol·L^{-1}) and NaOH (1

mol•L^{-1}) to check the chemical stability. The absorbance of resulting solution is used to evaluate the dissolved dyes (Fig. 12). Treated with ethanol, both of In-Hal and In-POS showed small absorbance, due to the low solubility of indigo into ethanol. Heated at high temperatures, In-Hal showed much higher absorbance than In-Hal-POS. In addition, with the increase of the heating temperature, more dye molecules dissolved into ethanol from heated In-Hal hybrid pigments. Although heated In-Hal-POS dissolved more dyes into ethanol than In-Hal-POS without heating, the maximum absorbance is only 0.2 (In-Hal-POS-190), much less than that of In-Hal-190 (0.9). Treated with HCl and NaOH, In-Hal hybrid pigments showed very low absorbance 550 nm to 650 nm. More important, nearly no absorbance occurred for In-Hal-POS hybrid pigments, demonstrating less dyes dissolving into the solutions.

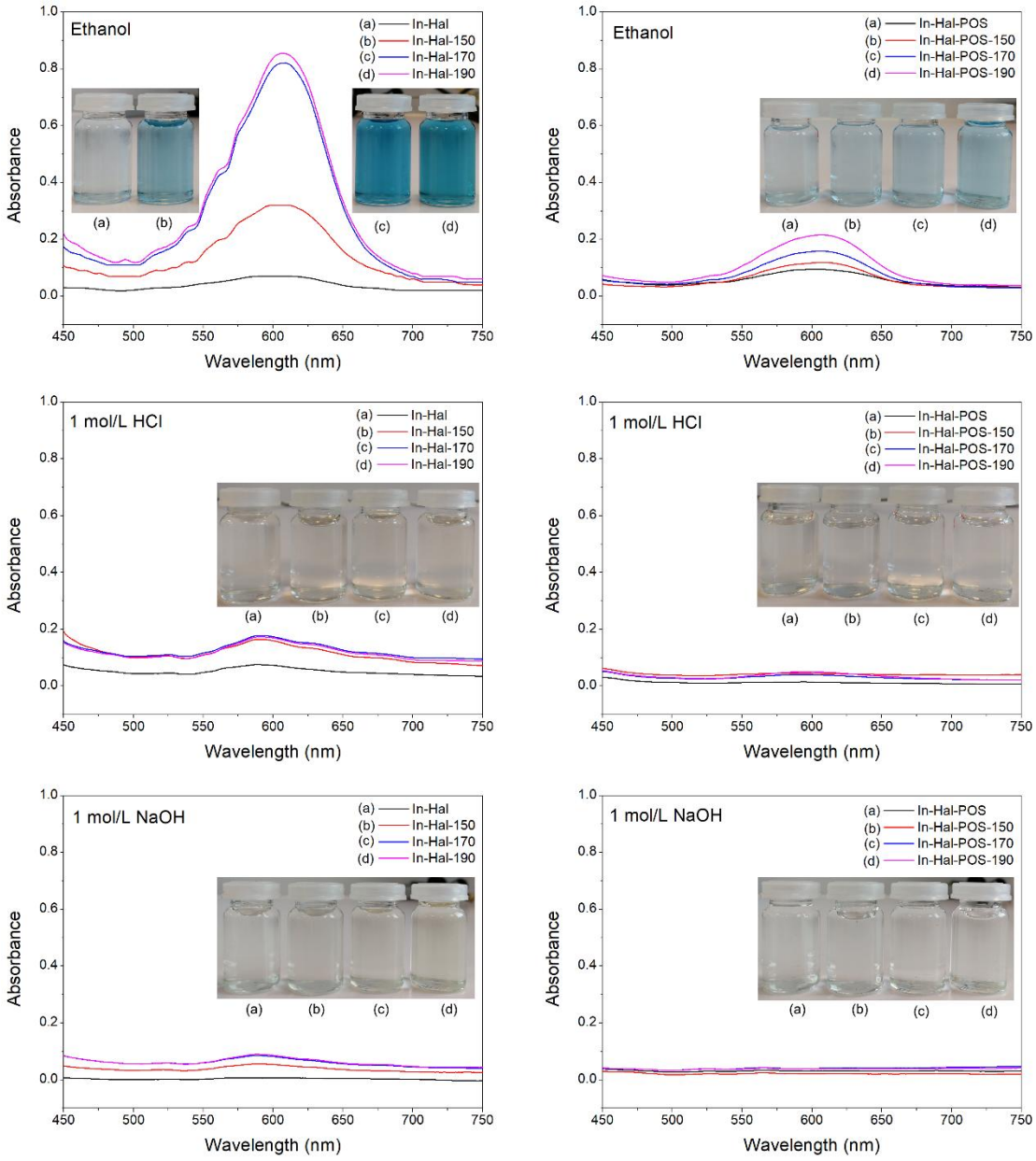

Fig. 12 Absorbance of resulting solutions derived from the ethanol, HCl and NaOH (left: hybrid pigments without POS, right: hybrid pigments with POS).

The solvent, acid and alkali may not only promote the dissolution of dye molecules into the liquid systems, but also interact with dye molecules, and finally result in the fading of the pigments. The digital pictures of hybrid pigments treated with ethanol, HCl and NaOH show different color changes (Fig. S1). For instance, In-Hal-190 treated with NaOH completely lost the blue color while the absorption of

resulting liquid is very low. The △E* values of hybrid pigments treated with different chemicals (Fig. 13) reveal the color change precisely. Treated with ethanol, In-Hal, In-Hal-150, In-Hal-170 and In-Hal-190 showed larger △E* values than the corresponding hybrid pigment with POS. Particularly, the solutions resulted from HCl and NaOH indicate low absorption for In-Hal and heated In-Hal hybrid pigments while the corresponding pigments exhibit high △E* values. For example, In-Hal-190 shows a △E* value of 10.3 after being treated with HCl and exhibits a △E* value of 30.4. On the contrary, the hybrid pigment with POS show a very low △E* value. This phenomenon testifies that covering with POS acts as a protective layer against chemical attacks, resulting in better chemical stability than hybrid pigments without POS.

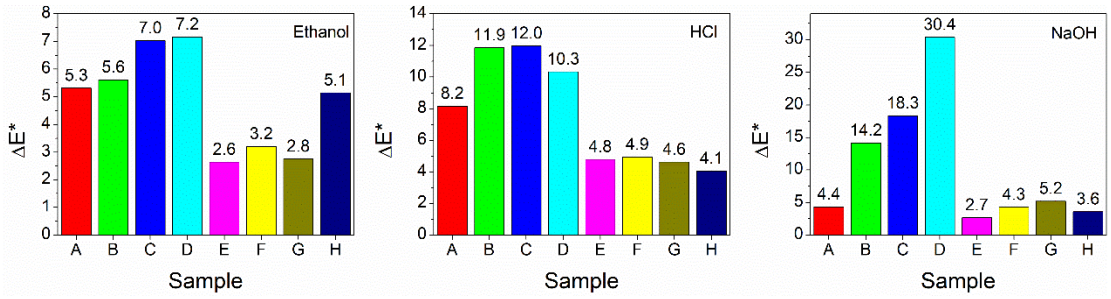

Fig. 13 A summary of the △E* values of hybrid pigments treated by ethanol, HCl and NaOH (A: In-Hal, B: In-Hal-150, C: In-Hal-170, D: In-Hal-190, E: In-Hal-POS, F: In-Hal-POS-150, G: In-Hal-POS-170, H: In-Hal-POS-190). The pigments heated at different temperatures (without treatment of ethanol, HCl and NaOH) are considered as the references.

3.6 Photostability

The hybrid pigments were continuously exposed under the visible light for 360 h to check the photostability. The △E* values of In-Hal, In-Hal-150, In-Hal-170 and In-Hal-190 (Fig. 14 (A)) increased rapidly with the increase of aging time. Finally, the △E* values reach 13.8 for In-Hal, 16.0 for In-Hal-150, 15.1 for In-Hal-170 and 18.7 for In-Hal-190 after fading for 360 h. However, the △E* values of In-Hal-POS hybrid pigments present much less increase with the treatment of visible light. After fading for 360 h, In-Hal-POS, In-Hal-POS-150, In-Hal-POS-170 and In-Hal-POS-190 exhibit the △E* values of 1.6, 2.2, 3.0 and 6.1. The digital pictures of hybrid pigments before and after treatment (inserted in Fig. 14) illustrate the similar results. Compared with In-Hal and heated In-Hal pigments, the hybrid pigments fade a lot after aging for 360 h. Pigments heated at higher temperatures tend to have more color changes after exposure under visible light, indicating that heating promotes the fading of indigo/halloysite pigments under visible light. In conclusion, the hybrid pigments with POS present better fastness.

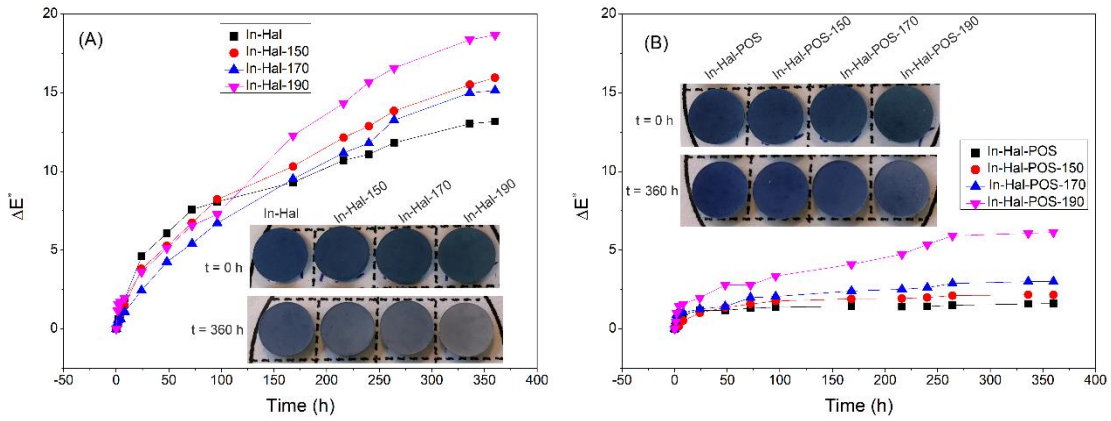

Fig. 14 Photostability of the hybrid pigments under visible light.

3.7 Discussion of the mechanism

The preparation of In-Hal-POS hybrid pigment can be described as showing in Fig. 15. By grinding method, the indigo molecules were dispersed on the external and inner surface of Hal, thus In-Hal hybrid pigment was obtained. Polycondensation happened between TEOS and HDTMS molecules, leading to the large protective layer covering on the surface of In-Hal. Because of the colorless and transparence of organosilane, no obvious effects on the color happen to the hybrid pigment with POS covering. However, the polarity of the pigment surface was totally changed due to the covering of POS layer. As presented in Fig. 16, Hal and In-Hal show the hydrophilic surface with low contact angle, since the hydrophilic Si-O and Si-OH groups on the surface of Hal. On the contrary, In-Hal-POS has a hydrophobic surface with the contact angle of 135°, implying a dense and continuous POS film on the surface. This POS film is stable even at high temperatures. When being heated at 150 °C, 170 °C and 190 °C, the contact angles of pigments nearly keep the same values, due to the excellent thermal stability of organosilane. This is in accordance with the TG result, which demonstrates the thermal decomposition of POS occurs above 300 °C.

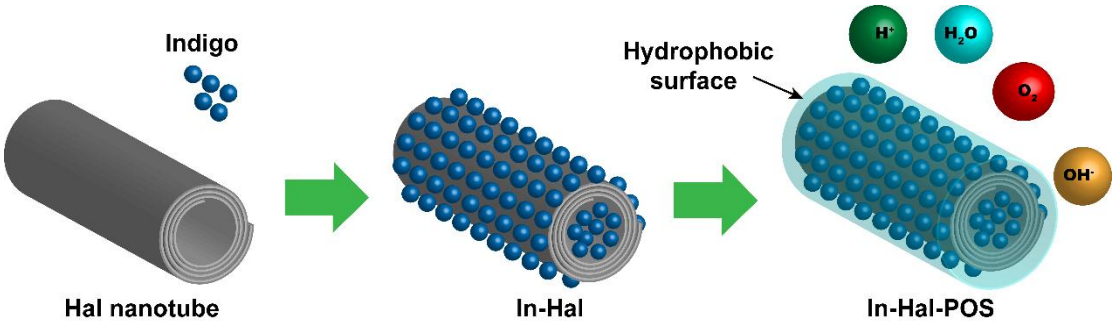

Fig. 15 Stabilization mechanism of hybrid pigments with the covering of POS layer.

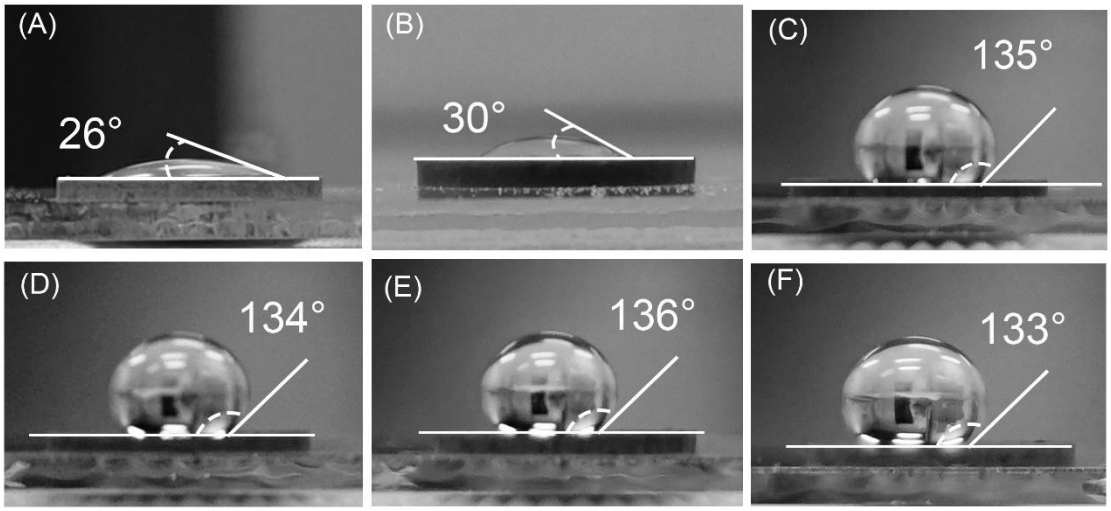

Fig. 16 Contact angle results of (A) Hal, (B) In-Hal, (C) In-Hal-POS, (D) In-Hal-POS-150, (E) In-Hal-POS-170 and (F) In-Hal-POS-190.

The color fading of pigment, in fact, is the chemical reaction between colorants with oxygen, water, acids, alkalis, etc. or dissolving into other solvents. Covered by POS, In-Hal hybrid pigment was packed, resulting in the insolation from chemicals outside. It is difficult for outside chemicals to enter and react with indigo dye, and also difficult for indigo molecules to move out and dissolve in water and other solvents. For example, when adding In-Hal and In-Hal-POS hybrid pigments in to the NaOH solution, In-Hal pigments immediately sunk to the bottom while In-Hal-POS pigments float on the top, without contact with NaOH solution (Fig. 17). After stirring, In-Hal pigments dispersed well in NaOH solution. But In-Hal-POS pigments still float on the top after stirring for 24 h, due to the hydrophobic surface. Thus, OH^- anions are

not easy to meet indigo molecules and react with them. It is similar for acid attack and organic solvents treatment. Usually, the fading of dyes can be considered as an oxidation process, which is affected by temperature, humidity, light, oxidant. Isolated from air (including oxygen, water, etc.), it is difficult for dye molecules to be oxidized.

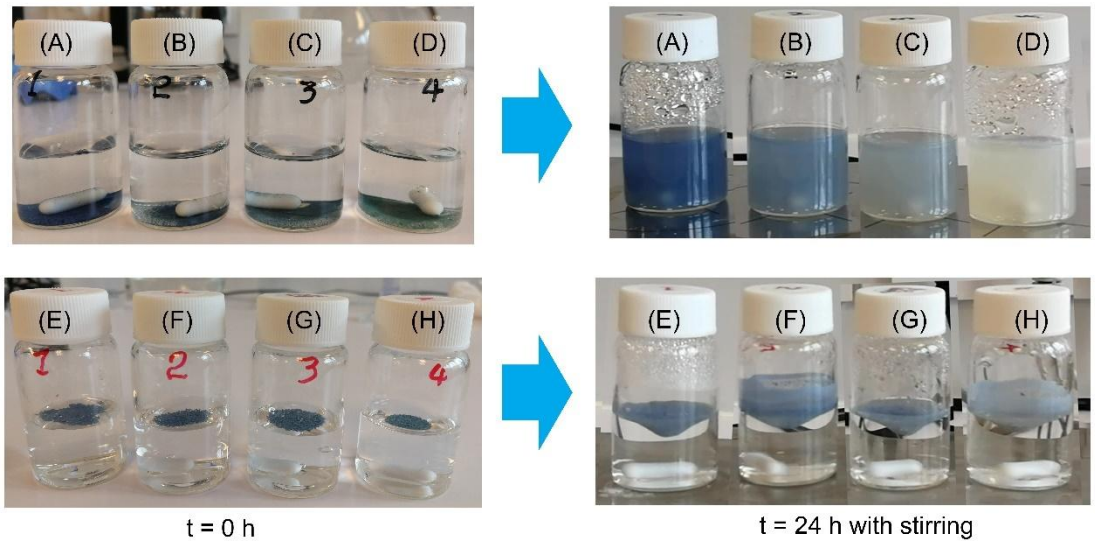

Fig. 17 Digital pictures of (A) In-Hal, (B) In-Hal-150, (C) In-Hal-170, (D) In-Hal-190, (E) In-Hal-POS, (F) In-Hal-POS-150, (G) In-Hal-POS-170 and (H) In-Hal-POS-190 treated with 1 mol•L^{-1} NaOH solution.

4. Conclusion

In this study, hybrid pigments based on Hal and indigo were prepared by grinding method. The chemical and thermal stability, and photostability of hybrid pigment with or without POS were comparatively investigated. Covering with POS layer was proved as an effective way to enhance the stability of hybrid pigments. Hybrid

pigments with POS presented excellent resistance to HCl (1 mol/L), NaOH (1 mol/L) and ethanol. The joint influences of heating and visible light exposure demonstrated that the POS layer also protected indigo from fading. Particularly, hybrid pigments with POS showed a maximum $\triangle E^*$ value of 6.1 while those without POS exhibited a maximum $\triangle E^*$ value of 18.6 when exposed under visible light illumination for 360 h (equals to 30 years in a common museum) What is more important, the interface interactions between indigo and Hal, POS and Hal have been revealed by FTIR and NMR. Indigo molecules immobilized on the Hal surface via hydrogen bonds, as well as Van der Waals force. POS layer was formed by polycondensation of organosilanes. POS not only simply covered on the surface, but also grafted with Hal surface. The covering of POS did not change the color obviously. Hybrid pigments tend to be greenish at high temperatures due to the oxidation of indigo. The POS layer enhanced the stability of hybrid pigments by forming a crosslinked film with hydrophobic surface (contact angle of about 135°). Consequently, dye molecules were packed on the Hal surface, resulting in excellent resistance to chemicals, heating and visible light. In summary, a new strategy to enhance the thermal stability and photostability of dye/clay hybrid pigments by covering with POS layer was verified. It is a promising method to produce durable organic-inorganic hybrid pigments. The grafting reaction of organosilanes with clay surface and the hydrophobicity play important roles in improving the stability of hybrid pigments. In the future work, the compatibility between this hybrid pigment and organic solvents, and the application in art works (e.g., oil paintings) should be attractive.

Acknowledgement

The support provided by China Scholarship Council (CSC) during the visit of Guanzheng Zhuang (No. 201706400010) to Sorbonne Université is acknowledged.

References

[1] A. Doménech, M.T. Doménech-Carbó, M.L.V. de Agredos Pascual, Chemometric study of Maya Blue from the voltammetry of microparticles approach, Analytical chemistry 79(7) (2007) 2812-2821.

[2] I.s.M. Leitão, J.S.r. Seixas de Melo, Maya Blue, an ancient guest–host pigment: synthesis and models, Journal of Chemical Education 90(11) (2013) 1493-1497.

[3] M.S.D. Río, A. Doménech, M.T. Doménech-Carbó, M. Suárez, E. García-Romero, Chapter 18 - The Maya Blue Pigment, Development in Clay Science, Elsevier Ltd 2011, pp. 453-481.

[4] G. Chiari, R. Giustetto, G. Ricchiardi, Crystal structure refinements of palygorskite and Maya Blue from molecular modelling and powder synchrotron diffraction, European Journal of Mineralogy 15(1) (2003) 21-33.

[5] B. Hubbard, W. Kuang, A. Moser, G.A. Facey, C. Detellier, Structural study of Maya Blue: textural, thermal and solidstate multinuclear magnetic resonance characterization of the palygorskite-indigo and sepiolite-indigo adducts, Clays & Clay Minerals 51(3) (2003) 318-326.

[6] M. José-Yacamán, L. Rendón, J. Arenas, M.C.S. Puche, Maya blue paint: an

ancient nanostructured material, Science 273(5272) (1996) 223.

[7] L.A. Polette, G. Meitzner, M.J. Yacaman, R.R. Chianelli, Maya blue: application of XAS and HRTEM to materials science in art and archaeology, Microchemical Journal 71(2) (2002) 167-174.

[8] D. Reinen, P. Köhl, C. Müller, The nature of the colour centres in 'Maya blue'—the incorporation of organic pigment molecules into the palygorskite lattice, Zeitschrift für anorganische und allgemeine Chemie 630(1) (2004) 97-103.

[9] A. Tilocca, E. Fois, The Color and Stability of Maya Blue: TDDFT Calculations, J Phys Chem C 113(20) (2009) 8683-8687.

[10] H. Van Olphen, Maya blue: a clay-organic pigment?, Science 154(3749) (1966) 645-6.

[11] L. Fan, Y. Zhang, J. Zhang, A. Wang, Facile preparation of stable palygorskite/cationic red X-GRL@ SiO 2 "Maya Red" pigments, RSC ADVANCES 4(108) (2014) 63485-63493.

[12] Y. Liu, Y. Kang, B. Mu, A. Wang, Attapulgite/bentonite interactions for methylene blue adsorption characteristics from aqueous solution, Chemical Engineering Journal 237 (2014) 403-410.

[13] R. Giustetto, O. Wahyudi, Sorption of red dyes on palygorskite: Synthesis and stability of red/purple Mayan nanocomposites, Microporous & Mesoporous Materials 142(1) (2011) 221-235.

[14] R. Giustetto, K. Seenivasan, D. Pellerej, G. Ricchiardi, S. Bordiga, Spectroscopic characterization and photo/thermal resistance of a hybrid palygorskite/methyl red

Mayan pigment, Microporous & Mesoporous Materials 155(11) (2012) 167-176.

[15] Y. Zhang, W. Wang, J. Zhang, P. Liu, A. Wang, A comparative study about adsorption of natural palygorskite for methylene blue, Chemical Engineering Journal 262 (2015) 390-398.

[16] Q. Wang, B. Mu, Y. Zhang, J. Zhang, A. Wang, Palygorskite-based hybrid fluorescent pigment: preparation, spectroscopic characterization and environmental stability, Microporous & Mesoporous Materials 224 (2015) 107-115.

[17] R. Giustetto, O. Wahyudi, I. Corazzari, F. Turci, Chemical stability and dehydration behavior of a sepiolite/indigo Maya Blue pigment, Appl Clay Sci 52(1-2) (2011) 41-50.

[18] S. Ovarlez, A.-M. Chaze, F. Giulieri, F. Delamare, Indigo chemisorption in sepiolite. Application to Maya blue formation, Comptes Rendus Chimie 9(10) (2006) 1243-1248.

[19] S. Ovarlez, F. Giulieri, A.M. Chaze, F. Delamare, J. Raya, J. Hirschinger, The Incorporation of Indigo Molecules in Sepiolite Tunnels, Chemistry - A European Journal 15(42) (2009) 11326-32.

[20] S. Ovarlez, F. Giulieri, F. Delamare, N. Sbirrazzuoli, A.M. Chaze, Indigo-sepiolite nanohybrids: Temperature-dependent synthesis of two complexes and comparison with indigo-palygorskite systems, Microporous & Mesoporous Materials 142(1) (2011) 371-380.

[21] C. Dejoie, P. Martinetto, E. Dooryhée, P. Strobel, S. Blanc, P. Bordat, R. Brown, F. Porcher, M.S.D. Rio, M. Anne, Indigo@Silicalite: a New Organic−Inorganic

Hybrid Pigment, Acs Appl Mater Inter 2(8) (2010) 2308-2316.

[22] F. Fournier, L.D. Viguerie, S. Balme, J.M. Janot, P. Walter, M. Jaber, Physico-chemical characterization of lake pigments based on montmorillonite and carminic acid, Appl Clay Sci 130 (2016) 12-17.

[23] A. Mahmoodi, M. Ebrahimi, A. Khosravi, H.E. Mohammadloo, A hybrid dye-clay nano-pigment: Synthesis, characterization and application in organic coatings, Dyes & Pigments 115(4) (2017) 811-815.

[24] S. Raha, N. Quazi, I. Ivanov, S. Bhattacharya, Dye/Clay intercalated nanopigments using commercially available non-ionic dye, Dyes & Pigments 93(1–3) (2012) 1512-1518.

[25] E. Joussein, Chapter 2 – Geology and Mineralogy of Nanosized Tubular Halloysite, Developments in Clay Science2016, pp. 12-48.

[26] T.F. Bate, Morphology and structure of endellite and halloysite, American Mineralogist 35 (1950).

[27] Churchman, G.J. Davy, T.J. Aylmore, L.A.G. Gilkes, R.J. Self, G. P., Characteristics of Fine Pores in Some Halloysites, Clay Miner 30(2) (1995) 89-98.

[28] Y. Zhang, L. Fan, H. Chen, J. Zhang, Y. Zhang, A. Wang, Learning from ancient Maya: Preparation of stable palygorskite/methylene blue@SiO 2 Maya Blue-like pigment, Microporous & Mesoporous Materials 211 (2015) 124-133.

[29] Y. Zhang, J. Zhang, A. Wang, Facile preparation of stable palygorskite/methyl violet@SiO2 "Maya Violet" pigment, Journal of Colloid & Interface Science 457 (2015) 254.

[30] J. Dong, Q. Wang, Y. Zhang, Z. Zhu, X. Xu, J. Zhang, A. Wang, Colorful Superamphiphobic Coatings with Low Sliding Angles and High Durability Based on Natural Nanorods, Acs Appl Mater Inter 9(2) (2016) 1941.

[31] J. Dong, J. Zhang, Photochromic and Super Anti-Wetting Coatings Based on Natural Nanoclays, Journal of Materials Chemistry A (2019).

[32] N. Tian, P. Zhang, J. Zhang, Mechanically Robust and Thermally Stable Colorful Superamphiphobic Coatings, Frontiers in chemistry 6 (2018).

[33] Y. Zhang, J. Zhang, A. Wang, From Maya blue to biomimetic pigments: durable biomimetic pigments with self-cleaning property, Journal of Materials Chemistry A 4(3) (2016) 901-907.

[34] P. Trigueiro, F. Rodrigues, B. Rigaud, S. Balme, J.-M. Janot, I.M. dos Santos, M.G. Fonseca, J. Osajima, P. Walter, M. Jaber, When anthraquinone dyes meet pillared montmorillonite: Stability or fading upon exposure to light?, Dyes and Pigments 159 (2018) 384-394.

[35] G. Zhuang, F. Rodrigues, Z. Zhang, M.G. Fonseca, P. Walter, M. Jaber, Dressing protective clothing: stabilizing alizarin/halloysite hybrid pigment and beyond, Dyes and Pigments 166 (2019) 32-41.

[36] P. Yuan, Chapter 7 – Thermal-Treatment-Induced Deformations and Modifications of Halloysite, Developments in Clay Science 7 (2016) 137-166.

[37] E. Joussein, S. Petit, J. Churchman, B. Theng, D. Righi, B. Delvaux, Halloysite clay minerals–a review, De Gruyter, 2005.

[38] E. Joussein, S. Petit, C.-I. Fialips, P. Vieillard, D. Righi, Differences in the

dehydration-rehydration behavior of halloysites: new evidence and interpretations, Clay Clay Miner 54(4) (2006) 473-484.

[39] P. Yuan, F. Bergaya, A. Thill, Chapter 1 – General Introduction, Developments in Clay Science 7 (2016) 1-10.

[40] P. Yuan, P.D. Southon, Z. Liu, M.E. Green, J.M. Hook, S.J. Antill, C.J. Kepert, Functionalization of halloysite clay nanotubes by grafting with γ-aminopropyltriethoxysilane, The Journal of Physical Chemistry C 112(40) (2008) 15742-15751.

[41] S. Hart, K.R. Koch, D.R. Woods, Identification of indigo-related pigments produced by Escherichia coli containing a cloned Rhodococcus gene, Microbiology 138(1) (1992) 211-216.

[42] S. Komarneni, C. Fyfe, G. Kennedy, Order-disorder in 1: 1 type clay minerals by solid-state 27 Al and 29 Si magic-angle-spinning NMR spectroscopy, Clay Miner 20(3) (1985) 327-334.

[43] R. Newman, C. Childs, G. Churchman, Aluminium coordination and structural disorder in halloysite and kaolinite by 27 Al NMR spectroscopy, Clay Miner 29(3) (1994) 305-312.

[44] S. Barrientos-Ramírez, G.M. de Oca-Ramírez, E. Ramos-Fernández, A. Sepúlveda-Escribano, M. Pastor-Blas, A. González-Montiel, Surface modification of natural halloysite clay nanotubes with aminosilanes. Application as catalyst supports in the atom transfer radical polymerization of methyl methacrylate, Applied Catalysis A: General 406(1-2) (2011) 22-33.

[45] P. Yuan, D. Tan, F. Annabi-Bergaya, Properties and applications of halloysite nanotubes: recent research advances and future prospects, Appl Clay Sci 112 (2015) 75-93.

[46] P. Luo, J.-s. Zhang, B. Zhang, J.-h. Wang, Y.-f. Zhao, J.-d. Liu, Preparation and characterization of silane coupling agent modified halloysite for Cr (VI) removal, Ind Eng Chem Res 50(17) (2011) 10246-10252.

[47] A.F. Peixoto, A.C. Fernandes, C. Pereira, J. Pires, C. Freire, Physicochemical characterization of organosilylated halloysite clay nanotubes, Micropor Mesopor Mat 219 (2016) 145-154.

[48] E. Abdullayev, A. Joshi, W. Wei, Y. Zhao, Y. Lvov, Enlargement of halloysite clay nanotube lumen by selective etching of aluminum oxide, ACS nano 6(8) (2012) 7216-7226.

[49] I.K. Tonlé, T. Diaco, E. Ngameni, C. Detellier, Nanohybrid Kaolinite-Based Materials Obtained from the Interlayer Grafting of 3-Aminopropyltriethoxysilane and Their Potential Use as Electrochemical Sensors, Chemistry of Materials 19(26) (2007) 23-29.

[50] Antonio Doménech, †, Dehydroindigo: A New Piece into the Maya Blue Puzzle from the Voltammetry of Microparticles Approach, Journal of Physical Chemistry B 110(12) (2006) 6027-39.

[51] Antonio Doménech, †, Indigo/Dehydroindigo/Palygorskite Complex in Maya Blue: An Electrochemical Approach, J.phys.chem.c 111(12) (2007) 4585-4595.

[52] H. Cheng, R.L. Frost, J. Yang, Q. Liu, J. He, Infrared and infrared emission

spectroscopic study of typical Chinese kaolinite and halloysite, Spectrochimica Acta Part A: Molecular and Biomolecular Spectroscopy 77(5) (2010) 1014-1020.

[53] H. Cheng, J. Yang, Q. Liu, J. Zhang, R.L. Frost, A spectroscopic comparison of selected Chinese kaolinite, coal bearing kaolinite and halloysite—A mid-infrared and near-infrared study, Spectrochimica Acta Part A: Molecular and Biomolecular Spectroscopy 77(4) (2010) 856-861.

[54] J. Theo Kloprogge, R.L. Frost, Raman microprobe spectroscopy of hydrated halloysite from a Neogene cryptokarst from Southern Belgium, Journal of Raman spectroscopy 30(12) (1999) 1079-1085.

[55] A. Amat, F. Rosi, C. Miliani, A. Sgamellotti, S. Fantacci, Theoretical and experimental investigation on the spectroscopic properties of indigo dye, Journal of Molecular Structure 993(1-3) (2011) 43-51.

[56] A. Baran, A. Fiedler, H. Schulz, M. Baranska, In situ Raman and IR spectroscopic analysis of indigo dye, Analytical Methods 2(9) (2010) 1372-1376.

[57] H. Pathak, D. Madamwar, Biosynthesis of indigo dye by newly isolated naphthalene-degrading strain Pseudomonas sp. HOB1 and its application in dyeing cotton fabric, Applied biochemistry and biotechnology 160(6) (2010) 1616-1626.